Proceedings of the 39th IAHR World Congress
19–24 June 2022, Granada, Spain
doi://10.3850/IAHR-39WC2521716X2022323

Computational Modeling of Coastal Flooding in Torquay due to Wave-Overtopping

Santiago Martelo[(1)], Aristos Christou [(2)], ,Shunqi Pan [(1)], Thorsten Stoesser[(2)], and Zhihua Xie [(1)]

[(1)] School of Engineering, Cardiff University, Cardiff, UK,
lopezsm@cardiff.ac.uk
pans2@cardiff.ac.uk
zxie@cardiff.ac.uk

[(2)] Department of Civil, Environmental & Geomatic Engineering, University College London, London, UK,
aristos.christou.18@ucl.ac.uk
t.stoesser@ucl.ac.uk

Abstract

A numerical study of the interaction of the current coastal defenses in Torquay (UK) is shown in this paper. Three-dimensional numerical simulations were carried out to assess the performance of coastal defenses and prevent excessive wave over-topping due to extreme weather events. The objective is to deliver the means to provide fast and reliable predictions when planning and designing coastal defenses by civil-engineering institutions and real-estate developers to prevent coastal flooding and subsequent disruption.
The computational fluid dynamic code Hydro3D is employed in this study, which has been validated and applied to many hydraulic engineering and marine renewable energy problems. Further refinements for the fluid-structure interaction (FSI) and free surface model are reported here. In this code the Eulerian fluid flow is solved through finite difference method with staggered arrangement of the velocity components on a Cartesian grid. The solution of a Poisson pressure-correction equation is achieved using the multi-grid technique in the final step as a corrector of the predicted velocities. In addition, this code was further enhanced with a local mesh refinement approach and a FSI model based on the Immersed Boundary Method (IBM). The evolution of the free surface is taken into account with the implementation of the Level Set Method (LSM).
Both the current IBM and a new FSI approach inspired on the Ghost Cell Method (GCM) have been tested using dam-break benchmark with an obstacle.

Keywords: Coastal defenses; Fluid-structure interaction; Turbulence; Two-phase flows.

1. INTRODUCTION

The research presented here tries to validate a simulation software as a reliable tool for assessing the performance of coastal defenses. As an example, a case study will take into account real wave conditions and the geometry of a sea wall in the Tor Bay Council. The ensuing sea level rise due to climate change is considered one of the mayor obstacles to overcome in the near future. Thus, having a design tool for assessing the performance of coastal defenses is a mayor asset for city councils in order to develop urban areas close to the shoreline and elaborate contingency plans against coastal flooding.
Hydro3D is the software employed in this research work and uses an improved version of the fluid-structure interaction model based on a Ghost Cell Method (GCM) resembling the ones described by Tseng & Ferziger (2003) and Mittal et al. (2008). Hydro3D is a solver for computational fluid dynamics based on finite differences. The former version of Hydro3D for studied the interaction between an immersed body and the fluid around employing the Immersed Boundary Method (IBM) developed by Can Kara (2015) which has been extensively validated for a wide range of Reynolds Numbers. However, it is hard to ensure the no slip and zero gradient boundary conditions on the surface of the immersed body, especially in two phase flows introducing a source of error as a result. The new model for fluid-structure interaction is based on the ghost-cell method which is known to work fairly well for high values of the Reynolds Number.

Another innovative approach is to combine the delta functions and Hp shape function for interpolating field values. It was found that the delta function yields better results at interpolating velocities for the ghost cell method. Although the interpolated values are above (bellow) the local maxima (local minima) using the delta functions helps to take into account the boundary layer effects while maintaining a sharp interface for a wide range of the Reynolds number. It was also found that the Hp shape functions performs better than the delta functions for interpolating pressure values.

In the next lines a formal description of the numeric algorithm will be presented for solving the fluid flow. Additionally, simulation results of a two*phase flow benchmark will be shown as well with the aim of validating Hydro3D. The final part of this work is the case study of the coastal flooding in the Tor Bay neighborhood of Tor Abbey in 2015.

2. METHODOLOGY

In this section the mathematical model for carrying out the fluid-structure simulations presented in this work is described.

2.1. Fluid Model

The model solves the 3D unsteady Navier-Stokes equations for a viscous in-compressible flow:

$$\frac{\partial u_i}{\partial x_i} = 0 \qquad [1]$$

$$\frac{\partial u_i}{\partial t} + \frac{\partial u_i u_j}{\partial x_j} = -\frac{1}{\rho}\frac{\partial p}{\partial x_i} + \frac{\partial}{\partial x_j}\left(\nu \frac{\partial u_i}{\partial x_j}\right) + D_i^{sgs} - g_i \qquad [2]$$

where equation [1] is the continuity equation and equation [2] is the vectorial momentum equation. The i and j indexes denote the 3-Dimensional Cartesian velocity components at their respective cell centers, p is the pressure, and ρ and ν are the fluid density and kinematic viscosity. Finally, g_i denotes Cartesian component of gravitational acceleration and the term D_i^{sgs}indicates additional subgrid scale stress forces that have been calculated using the Smagoringsky model, Smagorinsky (1963).

Hydro3D solves the Navier-Stokes equations in three dimensions which are integrated in time using a fractional step method. The spatial discretization uses a Cartesian grid for the pressure field and a staggered grid for the Cartesian velocity components. The continuity equation is present in the fractional step method when trying to solve for pressure in the final stage.

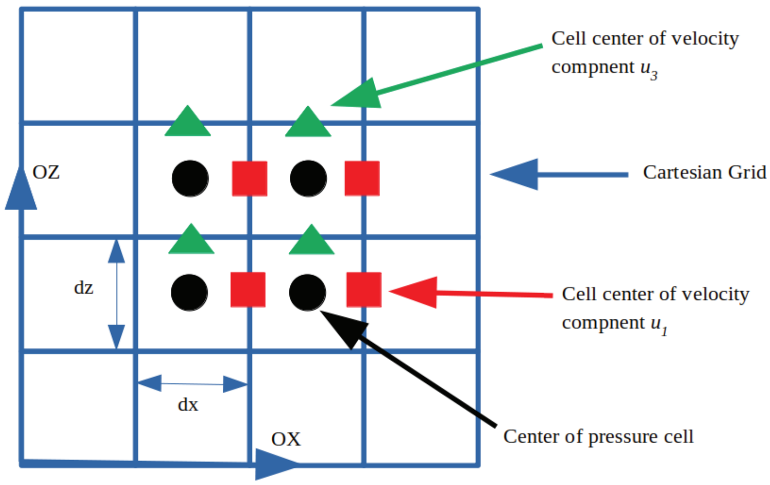

Figure 1. Cartesian grid.

In Figure 1 the black circles depict pressure cell centres at the centre of the blue cells. The red squares at the centre of the vertical faces represent the cell centres for velocity component u_1.The green triangles at the centre of the horizontal faces represent the cell centres for velocity component u_3.

In the fractional method (Van-Kan 1986), implemented in Hydor3D (Stoesser et al. 2008), first the convective and diffusive terms are estimated using the equation bellow:

$$\frac{u_i^* - u_i^{l-1}}{\Delta t} = -\alpha^l \left(\frac{\partial u_i u_j}{\partial x_j}\right)^{l-1} - \beta^l \left(\frac{\partial u_i u_j}{\partial x_j}\right)^{l-2} - \alpha^l \frac{1}{\rho}\frac{\partial p}{\partial x_i} \qquad [3]$$

$$+\alpha^l \frac{\partial}{\partial x_j}\left(\nu \frac{\partial u_i^{l-1}}{\partial x_j}\right) + \alpha^l D_i^{sgs} - \alpha^l g$$

where index l indicates field values of the previous time step. Coefficients α and β denote weights for the Runge-Kutta and Crank-Nicholson time-advancing schemes.

Finally, the Pressure Poisson Equation is solved using a multi-grid method. This equation derives from the continuity equation and a pseudo-pressure, p^s, is obtained by solving:

$$\frac{\partial}{\partial x_i}\left(\frac{1}{\rho}\frac{\partial p^s}{\partial x_i}\right) = \frac{1}{\alpha^l \Delta t}\frac{\partial u_i^*}{\partial x_i} \quad [4]$$

which allows to calculate a pressure and velocity corrections:

$$u_i^l = u_i^* - \alpha^l \Delta t \frac{\partial p^s}{\partial x_i} \quad [5]$$

$$p^l = p^{l-1} + p^s - \frac{\nu \alpha^l \Delta t}{2}\frac{\partial}{\partial x_i}\left(\frac{\partial p^s}{\partial x_i}\right) \quad [6]$$

2.2. Free Surface Model

The interface moves with the fluid particles and a pure advection equation can be used to model this effect (Sibel Kara 2014):

$$\frac{\partial \phi}{\partial t} + u_i \frac{\partial \phi}{\partial x_i} = 0 \quad [7]$$

where variable ϕ is the distance between the fluid particle and free surface or water-air interface. ϕ is positive for the water phase and negative for the air phase.

2.3. Fluid-Structure Interaction

A method that resembles the ghost cell method (GCM) is Gilmanov et al (2003), which presented a general reconstruction algorithm for simulating incompressible fluids applied to incompressible flows with complex immersed boundaries on Cartesian grids. In Balaras et al. (2004) eliminates the previously discussed ambiguities associated with interpolation along grid lines but its applicability is restricted to flows with immersed boundaries that are aligned with one coordinate direction (e.g., two-dimensional or axisymmetric shapes). In such cases, the solution reconstruction is greatly simplified as it needs to be performed in two-dimensional planes.

In Mittal et al. (2008) another immersed boundary method is described for simulating incompressible viscous flow past three-dimensional immersed bodies. It employs ghost cells for enforcing boundary conditions on the surface of the immersed body, that is, the immersed boundary. The complex body surface is represented by unstructured triangular elements and the flow is solved on non-uniform Cartesian grids.

In this work that model is applied to 2D flows and the immersed body is discretized using an unstructured triangular mesh where all the Cartesian grid nodes near the interface are identified. As the authors report, the solution at these nodes is reconstructed via linear interpolation along the local normal unit vector of the immersed body surface in such a way that the boundary conditions for pressure and velocity are enforced. The authors show that accuracy is of second order for laminar flows past a sphere.

In the original version of the ghost cell method implemented in Hydro3D the fractional scheme is also employed, but the additional term of the immersed force is not calculated. Basically, the main idea consists in selecting a set of ghost cells, that is, the Eulerian fluid cells inside the immersed body. After that, the mirror point with respect to the body surface is calculated. These ghost cells will need to be assigned u_i flow fields that cancel the respective mirror field values if one wants to apply a no-slip boundary condition for the velocities on the surface of a fixed body as describes this relationship:

$$u_i^{gh} = -u_i^{mr} \quad [8]$$

Where "gh" denotes field values in the ghost cell (fluid Eulerian cell inside the immersed body) and "mr" indicates the respective field values for the mirror image point. On the other hand, in order to apply zero-gradient boundary conditions on the body surface, the ghost cell value for pressure will be equal to the pressure magnitude at the mirror point:

$$p^{gh} = p^{mr} \quad [9]$$

In principle, after each velocity correction the ghost cell method is applied for the Cartesian velocity cell centers. Similarly, after the pressure correction this approach is applied to pressure cell centers inside the body. In llight of this, an algorithm for selecting cells inside bodies with closed cross-sectional shapes has been developed.

In order to estimate the value of the velocity and pressure at the mirror point various interpolation schemes have been considered. The first ones were the bi-linear scheme, a first order least squares method, delta functions and finally a tailored Hp interpolations scheme. These had good agreement with the results from the literature in low Reynolds conditions.

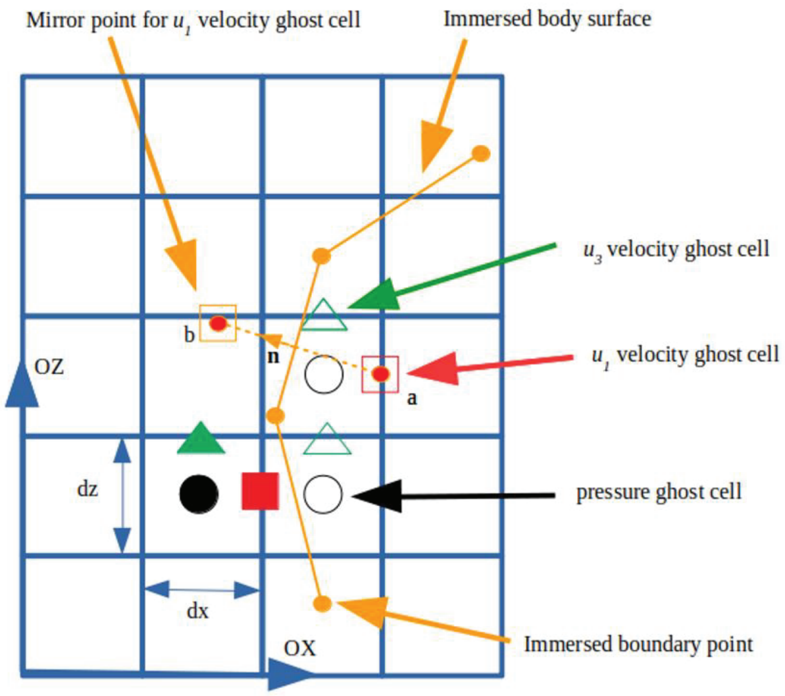

Figure 2. Cartesian grid with ghost cells

In Figure 2 the black hollow circles depict pressure ghost cell centres at the centre of the blue cells. The red hollow squares at the centre of the vertical faces represent the ghost cell centres for velocity component u_1. The green hollow triangles at the centre of the horizontal faces represent the ghost cell centres for velocity component u_3.

The location of each marker is given by the indexes of the cell faces downstream. This allows for an easy implementation of the ghost cell method since each marker is associated with the closest pressure and velocity cell faces.

2.4. Initial Conditions

For the initial conditions, the whole flow has to be given:

$$u_i(x, t = 0) = u_i^0(x) \quad [11]$$

Therefore, the initial pressure can be calculated based on the initial velocity field. Also, at time t =0 the location of the free surface is defined either because the initial wave and tide conditions are known:

$$\phi(x, t = 0) = \phi^0(x) \quad [12]$$

2.5. Boundary Conditions

Some boundary conditions need to be applied for solving the flow fields of staggered velocities, pressure and level set function $\boldsymbol{\phi}$.

2.5.1. *Boundary Conditions for Velocities*

For solid walls with no-slip condition it is needed that the fluid particle next to the boundary has the following velocity.

$$u_i^{gh} = 2u_i^{sb} - u_i^{mr} \quad [13]$$

where $\boldsymbol{u_i^{sb}}$ is the velocity of the solid boundary, a wall in this case. On the other hand, for modeling solid walls with free-slip if the wall stress effect is not significant and a coarse grid is used, the free slip boundary condition can be expressed as:

$$u_i^n = 0 \quad [14]$$

$$\frac{\partial u_n^T}{\partial n} = 0 \quad [15]$$

where $\boldsymbol{u_i^n}$ is the fluid velocity normal to the wall, $\boldsymbol{u_i^T}$ is the fluid velocity tangential to the wall and $\boldsymbol{n}$ is the normal direction to the wall.

On inlet surface boundaries Dirichlet Condition will be prescribed:

$$u_i^{gh} = u_i^{pr} \quad [16]$$

where $\boldsymbol{u_i^{pr}}$ is a prescribed velocity. In a similar way, at outlet surface one can prescribe either zero gradient for normal and tangential velocities or a Robin Boundary Condition. This alternatives are represented in the equations bellow:

$$u_i^{gh} = u_i^{mr} \quad [17]$$

$$u_i^{gh} = u_i^{mr} + \Delta t \frac{\partial u_i^{mr}}{\partial n} \quad [18]$$

2.5.2. *Boundary Conditions for Pressure*

For modeling solid walls Robin conditions are used to take into account the pressure drop across the immersed boundary:

$$p^{gh} = p^{mr} + \Delta t \frac{\partial p^{mr}}{\partial n} \quad [19]$$

For symmetry planes, inlets and outlets a zero gradient condition is employed.

$$p^{gh} = p^{mr} \quad [20]$$

2.5.3. *Boundary Conditions for level set method function* $\boldsymbol{\phi}$.

At solid walls and symmetry planes again zero gradient is prescribed

$$\phi^{gh} = \phi^{mr} \quad [21]$$

while at outlet and inlet walls a Dirictlet condition is used:

$$\phi^{gh} = \phi^{c} \quad [22]$$

3. NUMERICAL VALIDATION

The aim of this benchmark is to model the evolution of a column of water when it interacts with a vertical barrier. The vertical barrier spans along the OY direction of the frame of Cartesian reference in which the control volume was defined, from the South to the North boundaries which overlap with the domain walls in the y = 0m plane and y = 0.148 m plane, respectively. For this benchmark, the column of water was situated in the left part of the domain. To compare with other numerical and experimental results the control volume size employed was 200x50x200 cells. Figure 3 depicts the geometry of this case study.

Here the results are similar to the ones obtained with the IBM scheme with the advantage that there is no penetration of the water inside the structure and the zero gradient boundary condition for the ϕ variable of the Level Set Method is enforced.

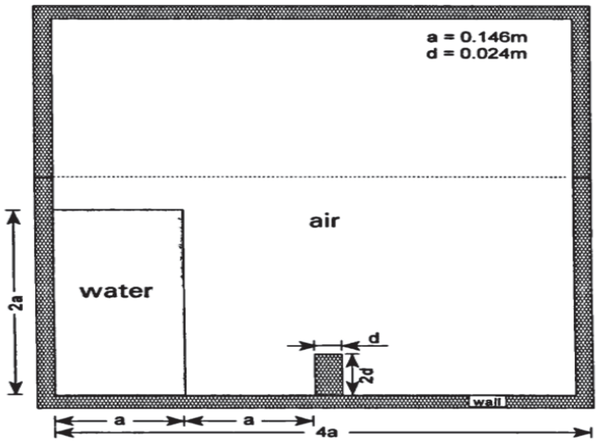

Figure 3. Initial location of water column and vertical barrier Ubink (1997).

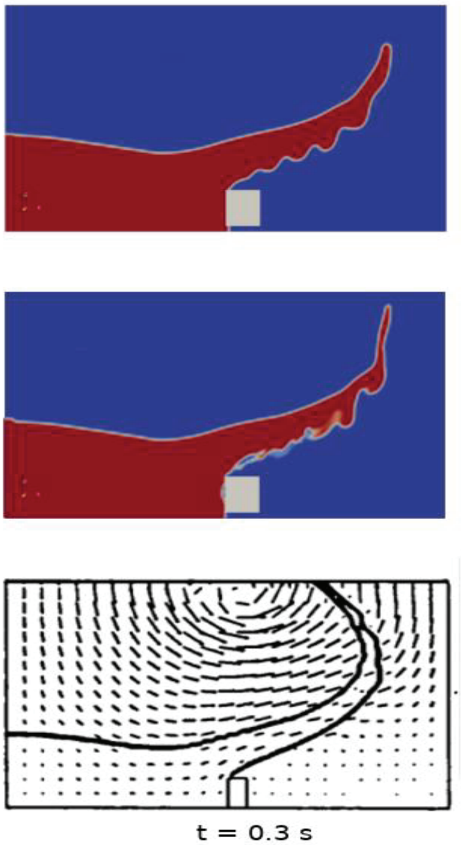

Figure 4. Evolution of the interaction of a water column with a vertical barrier.

Figure 4 presents the snapshots corresponding to times t = 0.3 s. On top is shown the outcome of using the Ghost Cell Method with bilinear interpolation in a grid of 200x200 cells. In the middle row it can be seen the results of the IBM scheme where a smooth delta function was employed. In the bottom row are presented the numerical results from Ubink (1997) employing a 200x200 mesh.

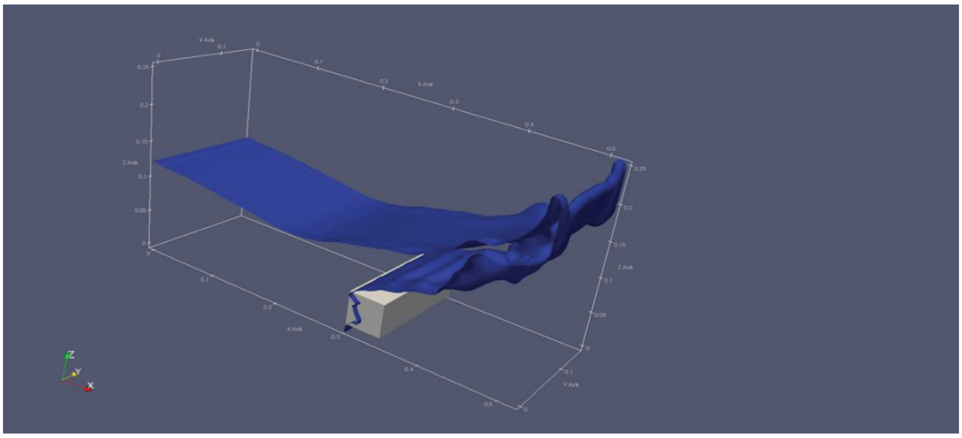

Figure 5. Colapsing of a water column with a vertical barrier at time t = 0.3s.

4. PRACTICAL CASE

In this section we will be showing simulations results of wave over-topping a real sea wall situated in the Tor Abbey, a neighborhood of Tor Bay Council. In the winter 2014 a mayor swell caused severe coastal flooding disruption costing the council around 500.000 GBP. For this reason we find relevant to evaluate if Hydro3D can replicate the behavior of this sea wall with the aim of using Hydor3D as a design tool to check the defectiveness of defenses of similar design.

The simulation will take as inputs the conditions of the flood alert for South Devon Coast on the 4th of February 2014, Torbay Flood Report (2004). The surge and tide at 21:46 pm raised the water level at 5.6 m above the Ordnance Datum (OD). The average wave height was 2.4 m with a peak of 3.7 m. The dimensions of the control volume for the simulation are a box of 48x3.6x19.2 m. A blueprint of the sea wall is presented in Figure 6:

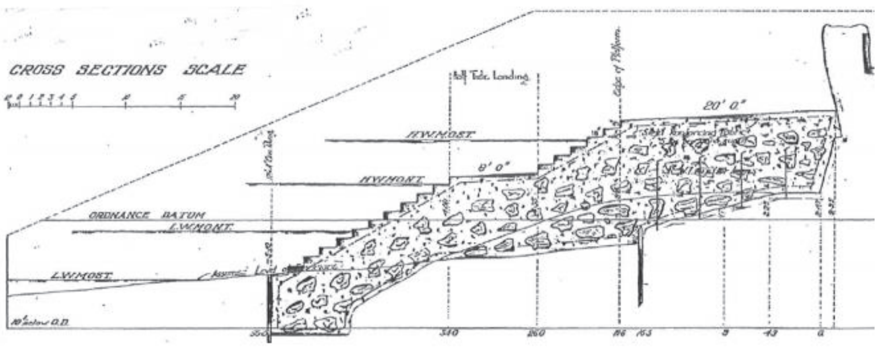

Figure 6. Sketch showing the characteristics of the sea wall located in the neighborhood of Tor Abbey in the Tor Bay Council.

The results of the simulation are showcased in the next series of pictures showing the numerical results the state of the free surface.

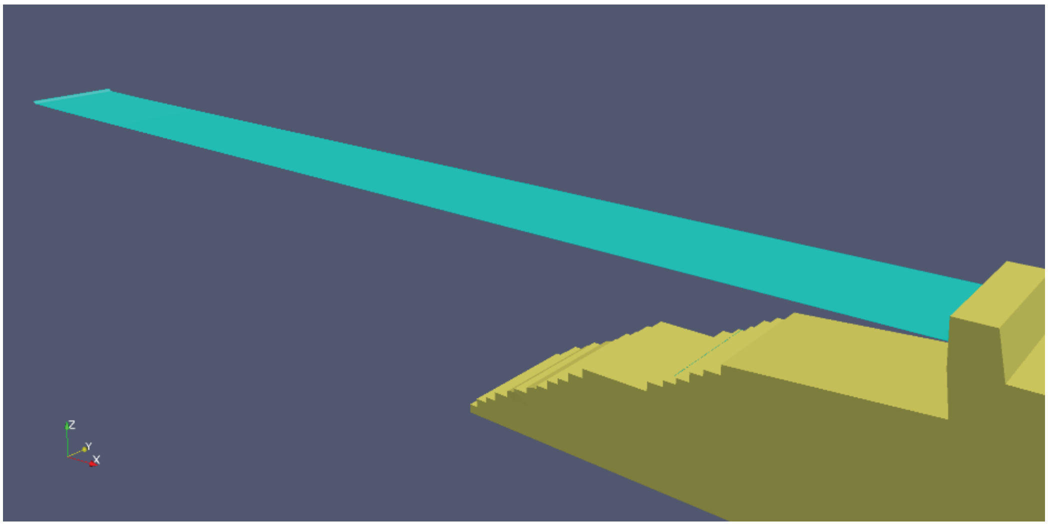

Figure 7. Evolution of the air-water interfase at time t = 0.25s.

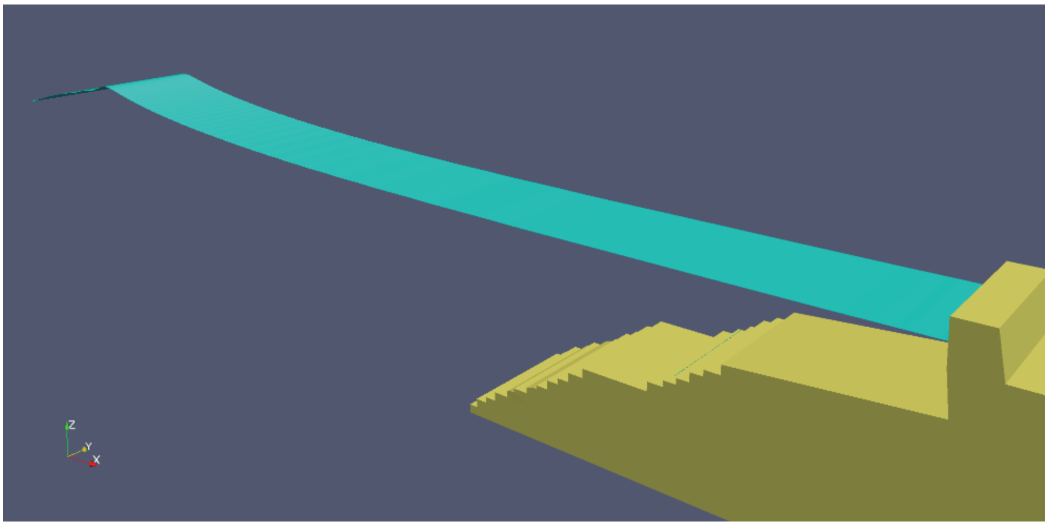

Figure 8. Evolution of the air-water interfase at time t = 2,5s.

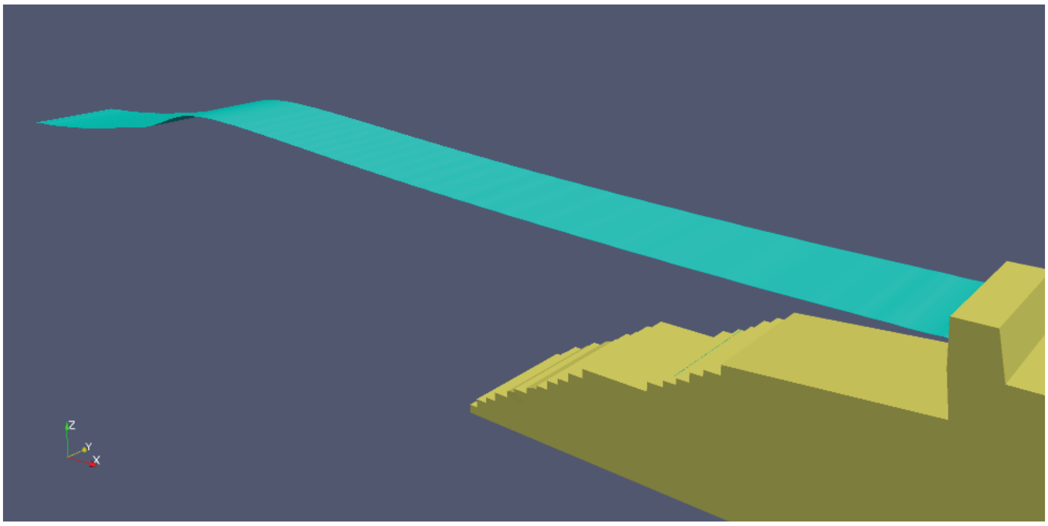

Figure 9. Evolution of the air-water interfase at time t = 3.75s.

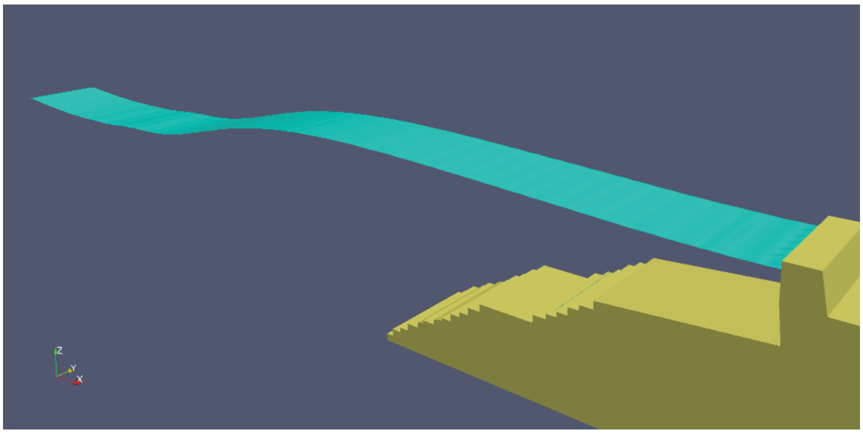

Figure 10. Evolution of the air-water interfase at time t = 5.00s.

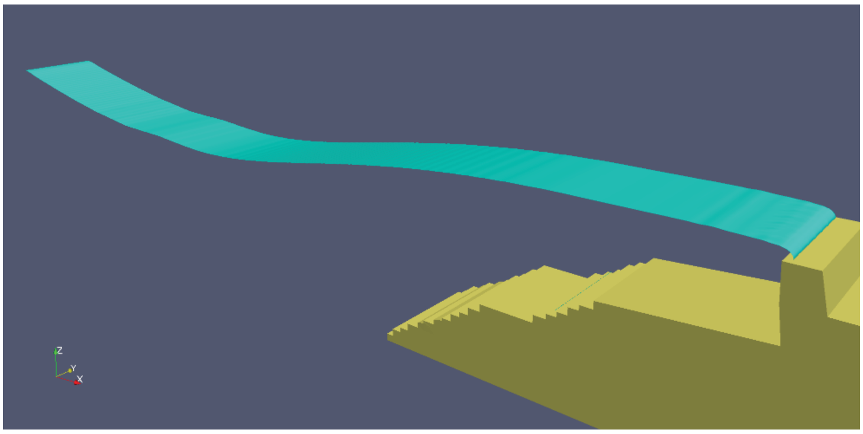

Figure 11. Evolution of the air-water interfase at time t = 6.25s.

5. CONCLUSIONS

Several authors have performed numerical experiments of breaking waves crashing against a wide range of coastal structures, namely: (Stansby 2016, Macabuag et al. 2018, Fuentes et al. 2019, Pappas et al 2021). Pappas et al. (2021) analyzed structural response of historic lighthouses to extreme wave impacts employing the Distinct Element Method (DEM). This work highlights that for same wave impact pulses, the shortened the wave duration the lower the overall structural displacement will be. In Macabuag et al. (2018) one can find a review of design tsunami design procedures and how they are included in US (ASCE 7-16) and Japaneese (MLIT 2570) standards. In Fuentes et al. (2019) a feasibility study of using a modified break-water dike for installation of a oscillating water column (OWC) wave energy converter is carried out. On the Stansby et al (2016) considered the overtopping of a coastal structure at laboratory scale by a solitary wave. Here the authors contrasted results with 3 models: 1D shallow-water-Boussinesq (SWB), the volume of fluid method (VOF) implemented in the finite volume software STAR-CD and also they employed a smoothed-particle-hydrodynamic (SPH) model. Wave breaking did not took place so the VOF results depended weakly on the turbulence model. The SWB showed some dependency on the friction coefficient and the SPH was inviscid since it was implemented with the Riemann formulation. Numerical simulations with the SWB model suggest that a coastal defense should be four times the height of an offshore wave amplitude to avoid overtopping. It was also observed that the SWB is only reliable for small slopes and wave amplitudes. In general it was also found that the SPH and SWB models yield results in close agreement with laboratory experiments and the VOF significantly underestimated overtopping.

The novelties introduced by Hydro3D are high fidelity simulations by means of employing a finite difference open-source code that uses both delta functions and Hp interpolation schemes for enforcing the boundary conditions of the GCM fluid-structure interaction model. It also has the capability of handling large geometries of solid bodies defined across several subdomains, helping to take advantage of FORTRAN parallel processing capabilities to expedite the results. Additionally, in this work a new fluid structure interaction model based on the ghost cell method (GCM) has been validated using the dam-break case. It also has been shown that Hydro3D can be used as a design tool to check the effectiveness of coastal defenses like sea walls.

Future work will be centered in validating the GCM in Hydro3D for moving objects in turbulent interfacial flows such as floating barges facing swells.

6. AKNOWLEDGEMENTS

The authors of this work are much obliged to the SPW High Performance Computer for providing training and the computational resources for carrying out the numerical simulations presented in the report.

Additionally, the authors would like to express their gratitude to Cardiff University and the UK Physical Research Council for providing funding to the WISE Doctoral Program, Grant Number: EP/L016214/1.

7. REFERENCES

Balaras, E. (2004). Modeling complex boundaries using an external force field on fixed Cartesian grids in large-eddy simulations. J. Comput. Phys 2004;33:375.

Fuentes M., Lara J., Rodriguez B., Gunache R. (2019). Physical and numerical modelling of a modified coastal dike for producing sustainable energy in harbors within the S@aports framework. XV Jornadas Españolas de Ingenieria de Costas y Puertos. May 2019.

Gilmanov, A., Sotiropoulos, F., Balaras, E. (2003). A general reconstruction algorithm for simulating flows with complex 3D immersed boundaries on Cartesian grids. Journal of Computational Physics 191 (2003) 660– 669A.

Kara, M. C., Stoesser and T. McSherry R. (2015). Calculation of fluidstructure interaction: methods, refinements, applications. Proc ICE – Eng Comp Mech 2015a; 168(2):59-78.

Kara, S., Kara, M. C., Stoesser, T. and Sturm, T. W. 2015. Free-surface versus Rigid-Lid LES computations for bridge-abutment flow. Journal of Hydraulic Engineering 141 (9), (ASCE)HY.1943-7900.0001028.

Papas A, D´Ayala D., Dassanayake D.T., Antonini A. and Hunt A. (2021). Rocking of offshore lighthouses under extreme wave impacts: Limit analysis, analytic formulations and distinct element method. Engineering Structures 228 (2021) 111534.

Macabuag J., Raby A., and Pomonis A. (2018). Tsunami design procedures for engineered buildings: a critical review. Proceedings of the Institution of Civil Engineers – Civil Engineering

Mittal, R., Dong, H., Bozkurttas, M., Najjar, F.M., Vargas, A., von Loebbecke, A. (2008). A versatile sharp interface immersed boundary method for incompressible flows with complex boundaries. J Comput Phys. 2008; 227(10): 4825–4852.

Smagorisnky J. (1963). General circulation experiments with the primitive equations. Mon Weather Rev 1963;91(3):99–164.

Stansby P., Xu R., Rogers B., Hunt A., Borthwick A. and Taylor P. (2008). Modelling tsunami overtopping of a sea defense by shallow-water Boussinesq, VOF and SPH methods. Flood Risk Management: Research and Practice (pp 251-261).

Stoesser, T. and Nikora V.I. (2008). Flow structure over square bars at intermediate submergence: large eddy simulation study of bar spacing effect. Acta Geophys 2008;56(3):876-93.

Tseng, Y.H. and Ferziger, J. (2003). A ghost-cell immersed boundary method for flow in complex geometry. Journal of Computational Physics, Vol 192, pp593-623.

Torbay City Council. (2015). Torbay Coastal Flood Event Data. 13/02/2015.

Ubbink, O. (1997). Numerical prediction of two fluid systems with sharp interfaces. Thesis submitted for the Degree of Doctor of Philosophy of the University of London and Diploma of Imperial College, 1997.

Van, Kan J. (1986). A second-order accurate pressure-correction scheme for viscous incompressible flow. SIAM J. Sci. Stat. Comput 1986;7:870.

